Rearrangement collisions in highly excited states of atomic hydrogen

N. C. Sil, B. C. Saha, H. P. Saha, and P. Mandal
Department of Theoretical Physics, Indian Association for the Cultivation of Science, Calcutta-700 032, India
(Received 4 August 1977; revised manuscript received 22 June 1978)

A new straightforward method for the evaluation of the rearrangement-scattering amplitude has been proposed to study the following reactions: $H^+ + H(1s) \rightarrow H(nlm) + H^+$; $e^+ + H(1s) \rightarrow (e^+e^-)\ (nlm) + H^+$, $2 \leq n \leq \infty$ and $l = 0,1$, in the first Born approximation embodying the full interacting potential. A contour-integral representation has been used for the Laguerre polynomial that occurs in the final-state wave function. The amplitude containing only the electron-nucleus interaction has been evaluated analytically. But the amplitude for the projectile nucleus interaction involves a contour integration on a circular path, and this integral can easily be evaluated numerically. To provide an estimate of the asymptotic cross section, expressions for the transition amplitudes when $n \rightarrow \infty$ have also been given. It is shown explicitly that the charge-exchange cross sections asymptotically obey the inverse n-cube law irrespective of the incident energy. In proton-hydrogen collisions our computed results for the low-lying discrete states show excellent agreement with the earlier theoretical values of Mapleton and those of Band as well. For positronium (Ps) formation all the reported results, except for the $2s$ excitation, are quite new. Zeros of the angular distributions are seen to be almost independent of the principal quantum number n, but dependent only on the projectile energy. $n^3\sigma$ shows regular smooth behavior with increasing n, and the results for $n = 18$ and $n \rightarrow \infty$ agree within 0.5% throughout the energy range considered.

I. INTRODUCTION

The problem of rearrangement collisions has drawn considerable attention of scientists in view of its connection with the explanation of various physical phenomena occurring in the planetary atmosphere, in supernova explosion in interstellar medium, in energetic solar flare, etc. In the neutralization of the charged particles that pass through gases, electron capture from the surrounding gas plays the most significant role. Capture takes place in the above cases either in the ground state or in the excited states. Investigation of the charge-exchange problem has received further impetus from the role it plays in the formation of the exotic atoms, such as positronium, muonium, protonium, etc. Highly excited hydrogen atoms can be formed by electron capture on protons accelerated to 25–100 keV in the laboratory. These highly excited atoms have a large number of unusual properties owing to their large size and small ionization potential. In addition to having an intrinsic interest of their own, these studies also find wide applications in radio astronomy, in plasma physics as well as in astrophysics.

The first quantum-mechanical treatment of the capture processes in ion-atom collisions is due to Oppenheimer.[1] Later Brinkman and Kramers[2] (BK) have further extended the investigation and evaluated by the first Born approximation (FBA), the cross section for the processes in which an ion captures in its $1s$ orbit an electron that was originally bound in the ground state of a hydrogen-like atom. They have carried out their calculations by neglecting the interaction between the incident ion and the nucleus since the contribution of this term to the capture cross section was expected to be of the order of the ratio m/M [(electron mass)/(proton mass)] as compared with the contribution of the electron-ion interaction. Bates and Dalgarno[3] and Jackson and Schiff[4] (JS) reconsidered the very same problem and have shown that the effect of the ion-nucleus interaction reduces the cross section considerably in better agreement with the observed values. With the increase of incident energy this reduction does not become vanishingly small. The ground-state capture problem has been studied more rigorously and more realistically by many workers.[5] Extension to a few low-lying excited states has also been made by some sophisticated methods[6] other than the Born approximation. An estimate of the order of magnitude of the asymptotic capture cross section has been given by Omidvar[7] using the FBA. Percival and Richard[8] more recently have used a variety of classical as well as semiclassical methods to study the electron-hydrogen atom and proton-hydrogen atom collisions to obtain excitation and charge-transfer cross sections.

When a positron, instead of an ion, is incident on an atom with sufficient energy, it has a fair possibility of capturing an atomic electron to form the light and large electron-positron atom, positronium (Ps). The pseudoatom of this electron-positron pair rotates around its common center of mass, held in dynamical equilibrium by a balance between the electrostatic attraction existing between the two charged particles of dissimilar nature and the centrifugal force present in the

rotatory motion. In gross electrical structure, a Ps atom resembles very closely the hydrogen atom in that both contain one positive and one negative particle. Positronium has been known for a long time to exist in excited states and many experimental attempts[9] have been made to study the properties of states of Ps with the principal quantum number $n>1$. Results, however, have been obtained only recently.[10] Though these results are not conclusive, they are highly interesting in that they give an estimate of the order of magnitude of the cross section.

In 1954 Massey and Mohr[11] emphasized for the first time the importance of the positron interaction for collision theory and considered for theoretical investigation the processes leading to the formation and subsequent dissociation of Ps. They computed in the FBA the ortho-Ps formation cross sections in the ground state as well as $2s$ excited states in a gas of atomic hydrogen. Omidvar[7] recently considered the asymptotic Ps formation using the FBA. Besides these two studies of the extreme cases for $n=2$ and $n\to\infty$, there exists, to our knowledge, no other theoretical calculations for the Ps formation in excited states.

In the present investigation we propose a new straightforward technique that will enable one to obtain the charge-exchange cross-section values without much effort in the framework of the FBA embodying the effect of the full interacting potential. We apply this method to compute FBA cross sections for the charge-transfer processes in proton–hydrogen-atom and for the Ps formation in positron–hydrogen-atom collisions where the final bound state is formed in an arbitrary excited ns or np state. For the charge-exchange collisions, whether the Born approximation appropriates the exact situation or not is indeed related to the convergence question. Calculations in the FBA however provide a good estimate of the cross section in many cases. Further it does not seem practicable to use more refined methods to treat the transitions to a highly excited state because of the fact that the final-state wave function has many oscillations.

The usual procedure to obtain scattering amplitudes for higher excited states is to generate an appropriate ground-state amplitude with suitable charge parameter and then to apply on it repeated parametric differentiations with respect to appropriate parameters. This is always encouraging only for some low-lying states. On the other hand, this procedure becomes tedious as well as intractable with the increase of the final principal quantum number n. The method as suggested here does not involve this type of parametric differentiation and enables one to obtain the cross-section values for arbitrary excited states without encountering the above difficulty.

The further motivation of the present work is to find out the asymptotic behavior of the capture cross sections with respect to n and is shown conclusively that as $n\to\infty$ the n^{-3} law is obeyed by the FBA cross section throughout the entire energy range.

The main outline of the paper is as follows: In Sec. II, we give first the general expression of the FBA scattering amplitude for charge transfer in arbitrary excited nlm states and then show the reduction of the integrals for proton–hydrogen-atom and positron–hydrogen-atom collisions for s-s and s-p transitions separately. The derivation of the asymptotic form of the scattering amplitude has been shown in Sec. III. Section IV deals mainly with the numerical procedure for the evaluation of the one-dimensional integral in the amplitude expressions for the projectile-nucleus interaction [see Eqs. (27), (37), etc]. We discuss there the numerical results thus obtained for the differential and total cross sections for the various transitions. Lastly we make our concluding remarks in Sec. V.

II. THEORY

A. General expression for the scattering amplitude

Let the incident particle B of mass M_B with charge Z_Be impinge on the target having an electron of mass m around the nucleus A of mass M_A with charge Z_Ae, e being the absolute value of the electronic charge. After collision the projectile B captures the electron from the target to form a bound state $(B+e)$ leaving the bare nucleus A alone. Let $\vec{k}_i$ and $\vec{k}_f$ denote, respectively, the initial and final momenta in the center-of-mass system. The conservation of energy then implies

$$k_i^2/2\mu_i+\epsilon_i=k_f^2/2\mu_f+\epsilon_f\,, \tag{1}$$

where μ_i and μ_f are, respectively, the reduced masses of the initial and final systems while ϵ_i and ϵ_f stand for the eigenenergies of the initial and final atoms.

In the framework of the Born approximation, the scattering amplitude for the rearrangement collisions can be written

$$g_{f\leftarrow i}(\hat{k}_f,\hat{k}_i) = -\frac{\mu_f}{2\pi}\int\Psi_f^*(\vec{r}_B,\vec{R}_2)V_{\rm int}(\vec{r}_A,\vec{R})\Psi_i(\vec{r}_A,\vec{R}_1)d\vec{r}_B\,d\vec{R}_2, \tag{2}$$

where

$$\Psi_i(\vec{r}_A,\vec{R}_1)=e^{i\vec{k}_i\cdot\vec{R}_1}\Phi_i(\vec{r}_A)$$

and (3)

$$\Psi_f^*(\vec{r}_B,\vec{R}_2)=e^{-i\vec{k}_f\cdot\vec{R}_2}\Phi_f^*(\vec{r}_B).$$

We take the post form of the interacting potential $V_{\rm int}$ which is a sum of the electron-nucleus and projectile-nucleus interaction as given by

$$V_{\rm int}=-Z_Ae/r_A+Z_AZ_Be^2/R. \tag{4}$$

Here $\vec{r}_A$ and $\vec{r}_B$ represent the position vectors of the electron with respect to the nucleus A and the projectile B, respectively (Fig. 1); $\vec{R}_1$ denotes the position vector of B with respect to the center of mass of the initial target atom and $\vec{R}_2$ that of the center of mass of the final atom from A. $\vec{R}$ represents the position vector of B with respect to A. $\Phi_i(\vec{r}_A)$ and $\Phi_f(\vec{r}_B)$ denote, respectively, the initial wave function of the target atom and the final wave function of the newly formed atom (atomic units will be used throughout the rest of the paper unless otherwise specified). Substituting Eqs. (3) and (4) in Eq. (2) one gets

$$g_{f\leftarrow i}(\hat{k}_f,\hat{k}_i)=-\frac{\mu_f}{2\pi}(I_{nlm}+J_{nlm}), \tag{5}$$

where

$$I_{nlm}=-\int F(\vec{r}_B,\vec{R}_2)\frac{1}{r_A}d\vec{r}_Bd\vec{R}_2, \tag{6a}$$

$$J_{nlm}=\int F(\vec{r}_B,\vec{R}_2)\frac{1}{R}d\vec{r}_Bd\vec{R}_2 \tag{6b}$$

with

$$F(\vec{r}_B,\vec{R}_2)=\exp(i\vec{k}_i\cdot\vec{R}_1-i\vec{k}_f\cdot\vec{R}_2)\Phi_i(\vec{r}_A)\Phi_f^*(\vec{r}_B). \tag{6c}$$

We confine ourselves to the problem of electron capture by a proton (or a positron) from the ground state of the target hydrogen atom to an arbitrary excited nlm state.

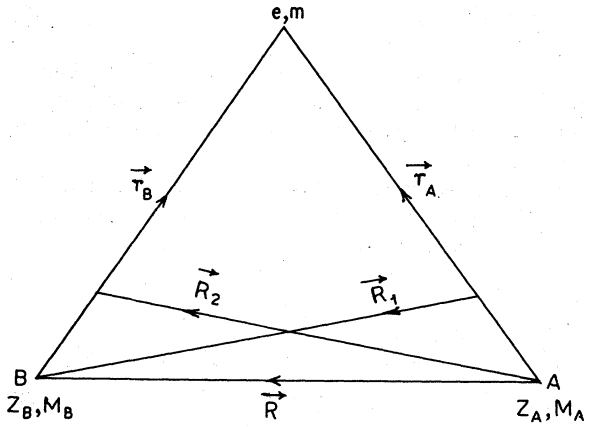

FIG. 1. Coordinate representation.

The initial ground-state wave function can be expressed

$$\Phi_i(\vec{r}_A)=N_ie^{-\gamma_1\vec{r}_A} \tag{7}$$

while the normalized final-state wave function $\Phi_f(\vec{r}_B)$ is given in spherical polar coordinates $(\vec{r}_B,\theta_B,\phi_B)$ by the following expression:

$$\Phi_f(\vec{r}_B)=N_{nlm}e^{-\gamma_nr_B}r_B^lL_{n+l}^{2l+1}(2\gamma_nr_B)\times P_l^m(\cos\theta_B)e^{\pm im\phi_B} \tag{8}$$

with the normalization constant

$$N_{nlm}=\left(\frac{(2l+1)(l-m)!}{4\pi(l+m)!}\right)^{1/2}\frac{(2\gamma_n)^{l+1}}{(n+l)!}\times\left(\frac{\gamma_n(n-l-1)!}{n(n+l)!}\right)^{1/2} \tag{9}$$

with $\gamma_n=\mu/n$ in which μ is the reduced mass (final state) which is 1 for the H atom and $\frac{1}{2}$ for the Ps atom. $P_l^m(x)$ is the associate Legendre polynomial of degree l and order m, and $L_{n+l}^{2l+1}(x)$ represents the associated Laguerre polynomial. We have used the following integral representation[12] of the Laguerre polynomial, which will help generate the rearrangement amplitude for any excited state in a convenient way:

$$L_a(x)=\frac{a!}{2\pi i}\oint_\Gamma\frac{e^{-xt/(1-t)}}{(1-t)t^{a+1}}dt, \tag{10}$$

where the contour includes the origin but does not enclose the point $t=1$. Differentiating under the integral sign in Eq. (10), one gets

$$L_a^b(x)=-\frac{a!}{2\pi i}\oint_\Gamma\frac{e^{-xt/(1-t)}}{(1-t)^bt^{a-b+1}}dt. \tag{11}$$

Making use of Eq. (11), the final-state wave function Φ_f [cf. Eq. (8)] takes the form

$$\Phi_{nlm}(\vec{r}_B)=-\frac{N_{nlm}}{2\pi i}\frac{(n+l)!}{2^{2l+1}}r_B^lP_l^m(\cos\theta_B)\times e^{\pm im\phi_B}\oint_\Gamma e^{-\gamma_\alpha r_B}\frac{(Z+1)^{n-l}}{(Z-1)^{n+l}}dZ \tag{12}$$

with

$$\gamma_\alpha=\gamma_nZ.$$

Here we have changed over to a new variable Z by the transformation

$$t=(Z-1)/(Z+1)$$

and with it, the pole has been shifted from the origin to the point $Z=1$ and the contour encloses only the point $Z=1$. On using Eqs. (7) and (12) in expressions (6a) and (6b), one gets

$$I_{nlm}=-\frac{N(nlm)}{2\pi i}\oint_\Gamma dZ\,\frac{(Z+1)^{n-1}}{(Z-1)^{n+1}}\int d\vec{r}_A\,d\vec{r}_B\exp(i\vec{k}_i\cdot\vec{R}_1-i\vec{k}_f\cdot\vec{R}_2-\gamma_\alpha r_B-\gamma_1 r_A)\,\frac{1}{r_A}\,r_B^l P_l^m(\cos\theta_B)e^{\pm im\phi_B} \tag{13}$$

and

$$J_{nlm}=\frac{N(nlm)}{2\pi i}\oint_\Gamma dZ\,\frac{(Z+1)^{n-1}}{(Z-1)^{n+1}}\int d\vec{r}_A\,d\vec{r}_B\exp(i\vec{k}_i\cdot\vec{R}_1-i\vec{k}_f\cdot\vec{R}_2-\gamma_\alpha r_B-\gamma_1 r_A)\,\frac{1}{R}\,r_B^l P_l^m(\cos\theta_B)e^{\pm im\phi_B}. \tag{14}$$

The subscripts nlm in I_{nlm} and J_{nlm} specify the final-state quantum numbers. The differential cross section for charge exchange is given by

$$\frac{d\sigma_{if}}{d\Omega}=\frac{\mu_i}{\mu_f}\frac{k_f}{k_i}\sum_{-l}^{l}|I_{nlm}+J_{nlm}|^2. \tag{15}$$

The total cross section is obtained by integrating the above expression over the entire solid angle.

B. Evaluation of the integrals J_{nlm} and I_{nlm}

We first consider the problem of proton–hydrogen-atom collisons and give the derivation of the integrals I_{nlm} and J_{nlm} for this case.

1. Proton-hydrogen atom collisions

(i) s-s transitions. For this case we have $l=m=0$ and thus Eq. (14) takes the form

$$J_{n00}=\frac{N(n00)}{2\pi i}\oint_\Gamma dZ\left(\frac{Z+1}{Z-1}\right)^n\int d\vec{r}_A\,d\vec{r}_B\exp(i\vec{k}_i\cdot\vec{R}_1-i\vec{k}_f\cdot\vec{R}_2-\gamma_\alpha r_B-\gamma_1 r_A)\,\frac{1}{|\vec{r}_A-\vec{r}_B|}. \tag{16}$$

Now, making use of the following Fourier transform

$$|\vec{x}-\vec{x}_1|^{-1}=(2\pi^2)^{-1}\int p^{-2}\exp[i\vec{p}\cdot(\vec{x}-\vec{x}_1)]\,d\vec{p}, \tag{17a}$$

and employing the following relations:

$$\vec{R}_1=[M_A/(M_A+1)]\vec{r}_A-\vec{r}_B\ \text{ and }\ \vec{R}_2=\vec{r}_A-[M_B/(M_B+1)]\vec{r}_B, \tag{17b}$$

we may write Eq. (16) as

$$J_{n00}=\frac{N(n00)}{2\pi i}\,\frac{1}{2\pi^2}\oint_\Gamma dZ\left(\frac{Z+1}{Z-1}\right)^n\int\frac{\exp[i(\vec{B}-\vec{Q})\cdot\vec{r}_A+i(\vec{Q}-\vec{C})\cdot\vec{r}_B-\gamma_\alpha r_B-\gamma_1 r_A]}{Q^2}\,d\vec{Q}, \tag{18a}$$

where

$$\vec{B}=[M_A/(M_A+1)]\vec{k}_i-\vec{k}_f\ \text{ and }\ \vec{C}=\vec{k}_i-[M_B/(M_B+1)]\vec{k}_f. \tag{18b}$$

After performing the radial integrations over r_A and r_B, one gets

$$J_{n00}=\frac{8N(n00)}{2\pi i}\,\frac{1}{\pi^2}\,\frac{\partial}{\partial\gamma_1}\oint_\Gamma dZ\left(\frac{Z+1}{Z-1}\right)^n\frac{\partial}{\partial\gamma_\alpha}M(\delta=0;\vec{B},\gamma_1;\vec{C},\gamma_\alpha), \tag{19}$$

where

$$M(\delta;\vec{B},\gamma_1;\vec{C},\gamma_\alpha)=\int\frac{d\vec{Q}}{(Q^2+\delta^2)(|\vec{B}-\vec{Q}|^2+\gamma_1^2)(|\vec{C}-\vec{Q}|^2+\gamma_\alpha^2)}. \tag{20}$$

The evaluation of the above integral has been carried out by Lewis[13] and is given by

$$M(\delta=0;\vec{B},\gamma_1;\vec{C},\gamma_\alpha)=\pi^2N^{-1/2}\ln\frac{\beta+N^{1/2}}{\beta-N^{1/2}}, \tag{21}$$

where

$$N=\beta^2-\alpha\gamma$$

with

$$\beta=\gamma_\alpha(B^2+\gamma_1^2)+\gamma_1(C^2+\gamma_\alpha^2)$$

and

$$\alpha\gamma=[|\vec{B}-\vec{C}|^2+(\gamma_1+\gamma_\alpha)^2](B^2+\gamma_1^2)(C^2+\gamma_\alpha^2). \tag{22}$$

The function $M(\delta=0;\vec{B},\gamma_1;\vec{C},\gamma_\alpha)$ as given by Eq. (21) is single valued and analytic even when we cross a branch cut of $N^{1/2}$. Substituting Eq. (21) in Eq. (19), we obtain

$$J_{n00}=-2i\frac{\gamma_n^{1/2}}{n}\frac{\partial}{\partial\gamma_1}\oint_\Gamma dZ\left(\frac{Z+1}{Z-1}\right)^n \times\left(\frac{\partial}{\partial Z}N^{-1/2}\ln\frac{\beta+N^{1/2}}{\beta-N^{1/2}}\right). \tag{23}$$

We would like to emphasize here that the study of the structure of the singularities of the Lewis function $M(\delta=0;\vec{B},\gamma_1;\vec{C},\gamma_\alpha)$ enables one to carry out the final contour integration over Z in a very elegant way. Keeping in mind that 0 and ∞ are the only singularities of the log function, we note that the Lewis function $M(0;\vec{B},\gamma_1;\vec{C},\gamma_\alpha)$ has singularities when $\alpha\gamma$ becomes zero. Under this consideration one obtains from Eq. (22) the following singular points for the function $M(0;\vec{B},\gamma_1;\vec{C},\gamma_\alpha)$:

$$Z_{1\pm}=\pm i|\vec{C}|/\gamma_n \tag{24a}$$

and

$$Z_{2\pm}=\pm i|\vec{B}-\vec{C}|/\gamma_n-\gamma_1/\gamma_n. \tag{24b}$$

Making use of the relation $B^2+\gamma_1^2=(C^2+\gamma_n^2)/\mu$ which follows from the conservation relation (1), one gets from Eq. (24a)

$$Z_{1\pm}=\pm i(1/\gamma_n)[(B^2+\gamma_1^2)\mu-\gamma_n^2]^{1/2}. \tag{25}$$

Thus

$$|Z_{1\pm}|\geq(n/\mu)(\mu-\mu^2/n^2)^{1/2},$$

since B^2 is a positive quantity. For the evaluation of the integral (23) the contour is to be chosen in such a way that the singularities $Z_{1\pm}$ and $Z_{2\pm}$ remain outside the path whereas only the singularity at $Z=1$ is included. For $n\geq 2$ we may choose a circular contour with radius r lying between 1 and $\frac{1}{2}n(4\mu-\mu^2)^{1/2}$ [the latter is obtained from Eq. (25) by putting $n=2$ under the radical sign]. Again from Eq. (24a) one gets

$$Z_{2\pm}=(|\vec{B}-\vec{C}|^2/\mu^2+\gamma_1^2n^2/\mu^2)^{1/2},$$

i.e., $|Z_{2\pm}|\geq n/\mu$, and this choice ensures our requirement that the points $Z_{2\pm}$ also are excluded.

Integrating by parts with respect to Z and noting that the first term being a single-valued and analytic function vanishes on the closed contour, Eq. (23) takes the form

$$J_{n00}=-4i\frac{\gamma_n^{3/2}}{\pi^2}n\mu\frac{\partial}{\partial\gamma_1}\oint_\Gamma dZ\frac{(Z+1)^{n-1}}{(Z-1)^{n+1}} \times M(0;\vec{B},\gamma_1;\vec{C},\gamma_\alpha). \tag{26}$$

Performing the parametric differentiation with respect to γ_1, one finally obtains

$$J_{n00}=-4i\frac{\gamma_n^{3/2}}{\pi^2}n\mu\oint_\Gamma dZ\frac{(Z+1)^{n-1}}{(Z-1)^{n+1}} \times M^{(\gamma_1)}(0;\vec{B},\gamma_1;\vec{C},\gamma_\alpha), \tag{27}$$

where

$$M^{(\gamma_1)}(0;\vec{B},\gamma_1;\vec{C},\gamma_\alpha) =-\frac{1}{2}\frac{N^{(\gamma_1)}}{N}M+\frac{\pi^2}{\beta^2-N}\left(\beta\frac{N^{(\gamma_1)}}{N}-2\beta^{(\gamma_1)}\right)$$

with

$$N^{(\gamma_1)}=-4\gamma_1[C^2(B^2+\gamma_1^2)-\vec{B}\cdot\vec{C}(C^2+\gamma_\alpha^2)]$$

and

$$\beta^{(\gamma_1)}=2\gamma_1\gamma_\alpha+(C^2+\gamma_\alpha^2);$$

the superscript (γ_1) denotes the differentiation with respect to γ_1.

In our actual calculations we have used $r=\frac{3}{4}n$. It is to be noted here that with the increase of n the radius also increases linearly. Using the transformation

$$Z=re^{i\theta}$$

the contour integration becomes an integral over θ having a range 0 to 2π. This has been evaluated numerically. It has been checked that the slight variation of the value of r within the allowed range does not change the results as expected.

In evaluating the integral I we take the Fourier transforms for $e^{-\gamma_1 r_A}$, $e^{-\gamma_\alpha r_B}$, and $1/R$. And making use of the relations (17b) and (18b) and performing the space integration, one gets from Eq. (13)

$$I_{n00}=\frac{8i}{\mu}\gamma_n^{5/2}\frac{1}{B^2+\gamma_1^2}\oint_\Gamma dZ\frac{\left(\frac{Z+1}{Z-1}\right)^n Z}{(C^2+\gamma_\alpha^2)^2}. \tag{28}$$

The integrand $f(Z)/(C^2+\gamma_\alpha^2)^2$ with

$$f(Z)=Z[(Z+1)/(Z-1)]^n$$

in the above equation has singularities at the point $Z=1$, a pole of order n and also at $Z=+i|\vec{C}|\gamma_n$, poles of order 2. We now verify that for a closed contour Γ_∞: $|Z|=R$, where $R\to\infty$

$$\oint_{\Gamma_\infty}\frac{dZ\,f(Z)}{(C^2+\gamma_\alpha^2)^2}=0, \tag{29a}$$

since

$$\left|\oint_{\Gamma_\infty}dZ\frac{f(Z)}{(C^2+\gamma_\alpha^2)^2}\right|\leq\frac{2\pi}{\gamma_n^4R^2}\to 0 \quad \text{as } R\to\infty. \tag{29b}$$

Our interest is to evaluate the integral over the

closed contour which encloses the lone singularity at $Z=1$. The poles at $Z=\pm i|\vec{C}|/\gamma_n$ of second order of the integrand in Eq. (28) lie, of course, outside it. Hence by Cauchy's residue theorem we have, in view of Eq. (29a),

$$\oint_\Gamma dZ\,\frac{f(Z)}{(C^2+\gamma_\alpha^2)^2} = -\frac{2\pi i}{\gamma_n^4}\sum(\text{residues of } f(Z) \text{ at } Z)=\pm i\,\frac{|\vec{C}|}{\gamma_n}. \tag{30}$$

We have thus avoided evaluating the residue of a function consisting of a pole of order n, and have, instead, evaluated the residues at poles of order 2 only. We thus finally obtain

$$\oint_\Gamma \frac{dZ f(Z)}{(C^2+\gamma_\alpha^2)^2} = -\frac{2\pi i n\gamma_n^3 Y}{|\vec{C}|(C^2+\gamma_n^2)} \tag{31}$$

with $Y=\sin(n\Theta)$

when

$$\Theta=\arctan\left(\frac{2|\vec{C}|\gamma_n}{C^2-\gamma_n^2}\right)+S\pi$$

where $S=0$ for $C^2-\gamma_n^2\geq 0$, and $S=1$ for $C^2-\gamma_n^2<0$. Substituting Eq. (31) in Eq. (28) the final expression for I_{n00} is obtained as

$$I_{n00}=16\pi^2\mu\gamma_n^{3/2}\,\frac{Y}{|\vec{C}|(B^2+\gamma_1^2)(C^2+\gamma_n^2)}. \tag{32}$$

(ii) s-p transitions. For $s\to p$ transitions, the value of the angular quantum number l must be 1 and the azimuthal quantum number $m=+1,0,-1$. Under these circumstances the integral I [Eq. (13)] and J [Eq. (14)] may be expressed

$$I_{n1m}=-\frac{N(n1m)}{2\pi i}\oint_\Gamma dZ\,\frac{(Z+1)^{n-1}}{(Z-1)^{n+1}}\int\int d\vec{r}_A\,d\vec{r}_B\exp(i\vec{k}_i\cdot\vec{R}_1-i\vec{k}_f\cdot\vec{R}_2-\gamma_\alpha r_B-\gamma_1 r_A)\frac{1}{r_A}r_B P_1^m(\cos\theta_B)e^{\pm im\phi_B} \tag{33}$$

and

$$J_{n1m}=\frac{N(n1m)}{2\pi i}\oint_\Gamma dZ\,\frac{(Z+1)^{n-1}}{(Z-1)^{n+1}}\int\int d\vec{r}_A\,d\vec{r}_B\exp(i\vec{k}_i\cdot\vec{R}_1-i\vec{k}_f\cdot\vec{R}_2-\gamma_\alpha r_B-\gamma_1 r_A)\frac{1}{R}r_B P_1^m(\cos\theta_B)e^{\pm im\phi_B}. \tag{34}$$

We choose the axis of quantization along the direction of the incident momentum $\vec{k}_i$. We first consider the case where $m=0$; Eqs. (33) and (34) take the form

$$J_{n10}=\lim_{\vec{\chi}\to 0}\frac{\partial}{\partial\chi_z}\frac{\partial}{\partial\gamma_1}\oint_\Gamma dZ\,\frac{(Z+1)^{n-1}}{(Z-1)^{n+1}}\frac{\partial}{\partial\gamma_\alpha}\times M(0;\vec{B},\gamma_1;\vec{C}',\gamma_\alpha), \tag{35a}$$

$$I_{n10}=\lim_{\vec{\chi}\to 0}\frac{\partial}{\partial\chi_z}\frac{\partial}{\partial\gamma_1}\oint_\Gamma dZ\,\frac{(Z+1)^{n-1}}{(Z-1)^{n+1}}\times\frac{1}{(C'^2+\gamma_\alpha^2)(B^2+\gamma_1^2)}, \tag{35b}$$

where $\vec{C}'=\vec{C}+\vec{\chi}$. It is of interest to note here that we have introduced a term $\exp(i\vec{\chi}\cdot\vec{r}_B)$ in expressions (35a) and (35b), and this, in turn helps us generate conveniently the term $r_B^l P_l^m(\cos\theta_B)e^{\pm im\phi_B}$ by repeated differentiation with respect to χ_x, χ_y, and χ_z; ultimately we let $\vec{\chi}\to 0$.

In deducing Eq. (35a) we have however made generous use of our previous results from Eqs. (17)–(22).

Here $M(0;\vec{B},\gamma_1;\vec{C}',\gamma_\alpha)$ is the Lewis function[13] as defined by Eq. (20) with the only difference that $\vec{C}$ has been redefined in the present case with an additional vector $\vec{\chi}$. It does not however change the basic properties of the function as such and the singularity structure remains unaltered on the whole.

Choosing the same contour $\Gamma: |Z|=n/\mu$ as before with the radius $n/\mu<|Z_{1\pm}|$ as given by Eq. (25), and following closely the deduction of the result in Eq. (23), one gets

$$J_{n10}=-\frac{16N(n10)}{2\pi i\gamma_n}\frac{\partial}{\partial\gamma_1}\oint_{\Gamma:|Z|=n}dZ\left(\frac{Z+1}{Z-1}\right)^n(Z-n)\times M(0;\vec{B},\gamma_1;\vec{C}',\gamma_\alpha). \tag{36}$$

Performing the differentiation with respect to γ_1, one has

$$\lim_{\vec{\chi}\to 0}\frac{\partial}{\partial\chi_z}J_{n10}=-\frac{16N(nl0)}{2\pi i\gamma_n}\oint_\Gamma dZ(Z-n)\left(\frac{Z+1}{Z-1}\right)^n M^{(\gamma Z)}(0;\vec{B},\gamma_1;\vec{C},\gamma_\alpha), \tag{37}$$

where $M^{(\gamma Z)}$ is defined as

$$M^{(\gamma Z)}=\lim_{\vec{\chi}\to 0}\frac{\partial}{\partial\gamma_1}\frac{\partial}{\partial\chi_z}M$$

and is given by

$$M^{(\gamma Z)}=\frac{\partial}{\partial\gamma_1}\left[-\frac{1}{2}\frac{N^{(Z)}}{N}M+\frac{\pi^2}{\beta^2-N}\left(\beta\frac{N^{(Z)}}{N}-2\beta^{(Z)}\right)\right], \tag{38}$$

in which the superscripts γ and Z represent the differentiation with respect to γ_1 and χ_z, respectively, and in the latter case the limit $\vec{\chi}\to 0$ is to be taken afterwards. For the evaluation of Eq. (38) one needs the following results:

$$\beta^{(\gamma_1)}=2\gamma_1\gamma_\alpha+C^2+\gamma_\alpha^2,\quad N^{(\gamma_1)}=-4\gamma_1[C^2(B^2+\gamma_1^2)-\vec{B}\cdot\vec{C}(C^2+\gamma_\alpha^2)],$$
$$\beta^{(Z)}=2\gamma_1|\vec{C}|C_Z,\quad N^{(Z)}=2C_Z(B^2+\gamma_1^2)[|\vec{C}|(B^2+\gamma_1^2)+2(C^2+\gamma_\alpha^2)(B^2-\vec{B}\cdot\vec{C})], \tag{39}$$
$$\beta^{(\gamma Z)}=2|\vec{C}|C_Z,\quad \beta^{(\gamma Z)}=-4\gamma_1\{|\vec{C}|C_Z[(B^2+\gamma_1^2)-\vec{B}\cdot\vec{C}]-B_Z(C^2+\gamma_\alpha^2)\}.$$

B_Z and C_Z are the Z components of $\vec{B}$ and $\vec{C}$ and are given from Eq. (19b) as

$$B_Z=\frac{M_A}{M_A+1}k_i-k_f\cos\theta_s$$

and

$$C_Z=k_i-\frac{M_B}{M_B+1}k_f\cos\theta_s,$$

θ_s being the scattering angle.

For the evaluation of the integral I_{n10} in Eq. (35b) we follow exactly the same procedure as in the case for the s-s transition and finally we obtain

$$I_{n10}=-i8\pi n^{-3/2}\left(\frac{3\mu}{1-1/n^2}\right)^{1/2}\frac{C_Z}{C^2(B^2+\gamma_1^2)}$$
$$\times\left(\frac{\sin(n\phi)}{|\vec{C}|}-\frac{2}{C^2+\gamma_n^2}[|\vec{C}|\sin(n\phi)+\mu\cos(n\phi)]\right), \tag{40}$$

where

$$\tan\phi=2|\vec{C}|\gamma_n/(\gamma_n^2-C^2).$$

For the m-degenerate states $m=\pm1$, the integrals $I_{n1,\pm1}$ as well as $J_{n1,\pm1}$ can be evaluated quite easily from Eqs. (35) by differentiating, instead of χ_z, with respect to χ_x and χ_y, and making use of the following relation

$$I_{n1,\pm1}=(1/\sqrt{2})(I_{n1x}\pm iI_{n1y}).$$

2. *Positron-hydrogen-atom collisions*

The scattering amplitude for Ps formation in either ns or np states may be obtained from Eqs. (13) and (14) by redefining only some of the quantities used earlier. For this case we have the projectile mass M_B = positron mass = 1 and the proton mass M_A is assumed to be infinitely heavy. We thus get $\vec{C}=\vec{k}_i-\frac{1}{2}\vec{k}_f$ and $\vec{B}=\vec{k}_i-\vec{k}_f$. $\gamma_n=\mu/n$ with $\mu=0.5$. Here the radius of the contour is chosen to be

$$r=n.$$

The expressions for I_{n00}^{Ps} and J_{n00}^{Ps} for the s-s transition may now be written

$$I_{n00}^{Ps}=-\frac{4\gamma_n^{1/2}}{2\pi i\pi^2}\oint_{\Gamma;|Z|=n}dZ\,\frac{(Z+1)^{n-1}}{(Z-1)^{n+1}}$$
$$\times M^{(\gamma_1)}(0;\vec{B},\gamma_1,\vec{C},\gamma_\alpha), \tag{41a}$$

$$J_{n00}^{Ps}=\frac{4\mu^{3/2}Y}{n^{3/2}|\vec{C}|(B^2+\gamma_1^2)(C^2+\gamma_\alpha^2)}. \tag{41b}$$

III. ASYMPTOTIC FORM OF THE SCATTERING AMPLITUDES

It is of great interest to study the behavior of the Born cross section for electron capture into excited ns and np states when $n\to\infty$ by protons and positrons from the ground state of the hydrogen atom.

With the increase of the principal quantum number n one gets

$$\lim_{n\to\infty}\gamma_n=\lim_{n\to\infty}\mu/n=0.$$

It is also apparent that on the contour where $Z=re^{i\theta}$, γ_α becomes independent of n since

$$\gamma_\alpha=\gamma_nZ=\mu e^{i\theta}.$$

Moreover, the Lewis function $M(0;\vec{B},\gamma_1;\vec{C},\gamma_\alpha)$ in this consideration has no explicit dependence on n, except through $\vec{B}$ and $\vec{C}$ only. Again, in the limit $n\to\infty$, the weight factor $[Z+1)/(Z-1)]^n$ becomes $e^{2\delta}$ with $\delta=\mu e^{-i\theta}$. Thus we may rewrite Eqs. (32) and (27) in the form

$$\lim_{n\to\infty}(n^{3/2}I_{n00}^H)=16\pi\sin(2/|\vec{C}|)/|\vec{C}|^3(B^2+\gamma_1^2), \tag{42a}$$

and

$$\lim_{n\to\infty}(n^{3/2}J_{n00}^H)$$
$$=-\frac{4\nu}{\pi^2}\int_0^{2\pi}d\theta\exp[2\nu\cos\theta-i(\theta+2\nu\sin\theta)]$$
$$\times M\left(0;\vec{B},\gamma_1;\vec{C},\frac{e^{i\theta}}{\nu}\right). \tag{42b}$$

with

$$\nu=1/\mu.$$

Similarly Eqs. (36) and (40) for the s-p transition may be expressed

$$\lim_{n\to\infty}(n^{3/2}I^H_{n10}) = \frac{4\pi C_Z}{C^2(B^2+\gamma_1^2)}\left(\frac{\sin\phi}{|\vec{C}|}+\frac{2}{C^2}(|\vec{C}|\sin\phi+\mu\cos\phi)\right) \tag{43a}$$

and

$$\lim_{n\to\infty}(n^{3/2}J^H_{n10}) = -\frac{\mu}{\pi^2\nu^2}\int_0^{2\pi}(e^{2i\theta}-e^{i\theta})e^{2\omega} \times M^{(\gamma Z)}(0;\vec{B},\gamma_1;\vec{C},\mu e^{i\theta})d\theta\,, \tag{43b}$$

where $\omega=\nu e^{-i\theta}$ and $\phi=2\mu/|\vec{C}|$.

For positron-hydrogen scattering the expressions for the scattering amplitudes in s-s transitions for the asymptotic case when $n\to\infty$ may be readily obtained by making the relevant changes in Eqs. (41a) and (41b) as well.

IV. RESULTS AND DISCUSSION

The results of our numerical calculations of the differential as well as integrated cross sections for electron capture in arbitrary excited ns and np states by protons as well as by positrons from the ground state of hydrogen atom have been presented.

A. Numerical procedure

For the evaluation of J_{nlm} we note that the real part of the integrand is symmetric about the real axis and the imaginary part is antisymmetric in the s-s transition while for the s-p transition these features are reversed. Thus in actual calculations we need only consider the range of integration of θ from 0 to 2π. The Gaussian quadrature method is employed after dividing the range of integration 0 to π into four equal intervals. Convergence for each part has been tested by increasing the number of Gaussian points.

The total cross section has been obtained numerically using the Gaussian quadrature method. In ion-atom collisons, except at very low velocities, the main contribution to the total cross section comes from the forward direction and the angular spread of the scattering amplitudes decreases with the increase of the projectile energy. Keeping these facts in mind, we have used, in the $H^+ - H$ collision, Z as our integration variable instead of the scattering angle, where Z is related to θ_s by the following transformation

$$\theta_s=\cos^{-1}\left[1-\frac{1}{k_i^2}\left(\frac{1+Z}{1-Z}\right)\right].$$

In the positron-atomic-hydrogen collision we have used $\cos\theta_s$ as the integration variable. The convergence of the results has been tested by increasing the number of Gaussian points.

As a numerical check on our general programs we have compared our computed cross-section results for the low-lying states for s-s as well as s-p transitions with the corresponding values obtained by Mapleton[14] using the FBA and have found that they agree with Mapleton's results up to all three significant digits as given by him at all available energies. Moreover, the FBA values of Band[15] for the electron capture into states $13p$ and $14p$ agree quite nicely with our results. For example, at an incident energy of 50 keV, Band's results for $n=13$ and $n=14$ are 0.134×10^{-2} and 0.103×10^{-2} in units of a_0^2, respectively, whereas our findings are $0.130\times10^{-2}a_0^2$ and $0.104\times10^{-2}a_0^2$. Similar agreement of our results with Band's FBA values is found to occur for the ns capture also.

B. Differential cross sections

1. s-s transition

In Fig. 2 differential cross section for the electron capture into the $2s$ state of the hydrogen atom

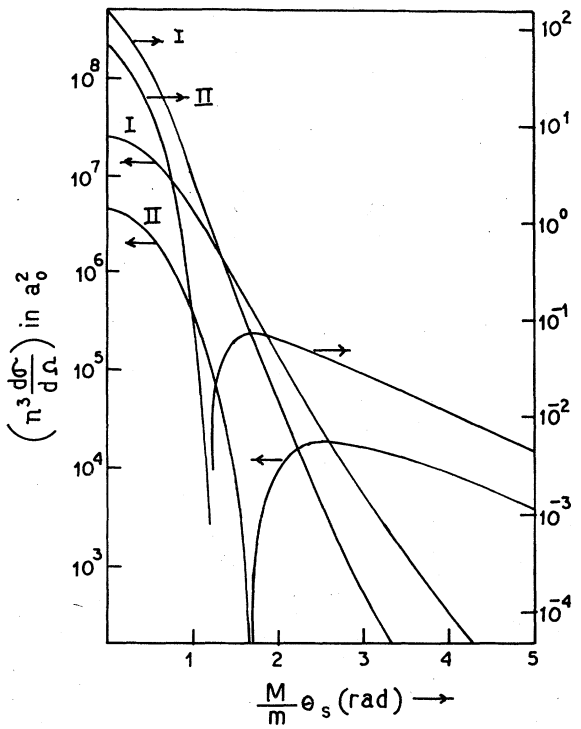

FIG. 2. n^3 differential cross section for the electron capture into the $2s$ state of the hydrogen atom at $E=50$ keV and 1 MeV (in laboratory system). The scattering angle θ_s is multiplied by ratio of the proton to electron masses. The solid curves represent the present results, employing the BK approximation (I) and the JS approximation (II) as well.

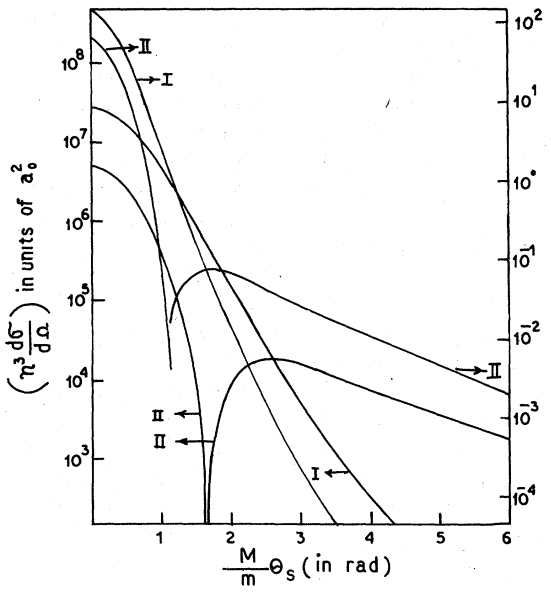

FIG. 3. Notations are same as in Fig. 2, but the capture takes place into the 6*s* state.

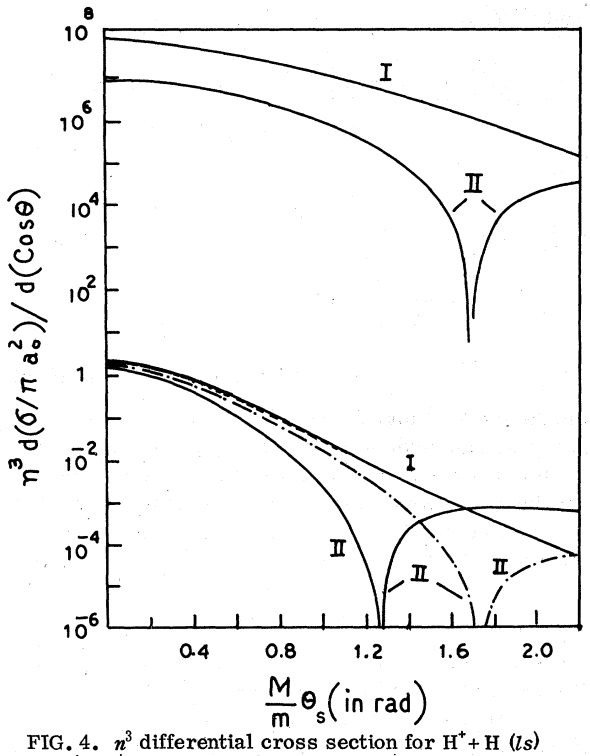

FIG. 4. n^3 differential cross section for $H^+ + H$ $(1s)$ $\rightarrow H(ns) + H^+$ when $n \rightarrow \infty$ for the small scattering angles at $E = 50$ keV and 2.5 MeV. Notations are the same as for Fig. 2 except the chain curve refers to the asymptotic values of Omidvar (Ref. 7).

for the incident energies 50 and 1000 keV are plotted against the scattering angle θ_s. From the figure it is evident that the BK curve decreases monotonically from a sharp peak in the forward direction with the increase of the scattering angle. The JS curve, on the other hand, falls off very rapidly from a peak value in the forward direction and becomes zero at an angle θ_0. It again rises to a maximum and then falls off monotonically. The BK peak in the forward direction is always higher than the corresponding JS peak. For the incident energy $E = 50$ keV the JS cross section becomes zero around the scattering angle $(M/m)\theta_0 = 1.65$. The position of the zero is shifted towards the forward direction $[(M/m)\theta_0 = 1.2]$ with the increase of the incident energy ($E = 1000$ keV). The origin of the zero is the JS differential cross section is due to the fact that the contributions to the amplitude from the attractive and repulsive potentials that occur as sum in JS, are always real but opposite in sign. At some scattering angle these contributions become equal in magnitude, as a result the sum becomes zero.

Figure 3 represents the present results for $n = 6$ for the incident energies 50 and 1000 keV. A relative comparison between the Figs. 2 and 3 reveals that the position of the zero of the JS curve for $E = 50$ keV and $E = 1000$ keV are almost identical with the corresponding zero points for $n = 2$. (Fig. 2). It is evident from the figure that in this case also the position of the zero at 1000 keV is shifted from the corresponding zero position at 50 keV towards the zero-degree scattering angle. It has been observed that at a fixed incident energy the zero position for any higher excited state remains almost the same irrespective of the value of the principal quantum number n. Here we would like to mention that the peak in the forward direction becomes sharper with the increase of the incident energy and the maximum contribution to the total cross section comes from the range 0 to θ_0 of the scattering angle.

In Fig. 4 we have shown the present asymptotic values $(n \rightarrow \infty)$ of the differential cross section for the incident energy 50 keV and 2.5 MeV. Recently calculated values for the asymptotic cross section at $E = 2.5$ MeV due to Omidvar have also been displayed in the same figure for comparison. It is apparent from the figure that the present BK curve is indistinguishable from the corresponding BK curve of Omidvar[7] throughout the angular range considered, whereas there is a marked disagreement between the present JS results and the corresponding JS results of Omidvar. The zero position of the differential cross section of these two JS curves are quite different. Figures 2 and 3 shows that with the increase of the incident energy the zero position in the differential cross section is shifted towards the origin for $n = 2$ and 6. Similar feature is also apparent in Fig. 4. This feature is also noted in Fig. 5 where the

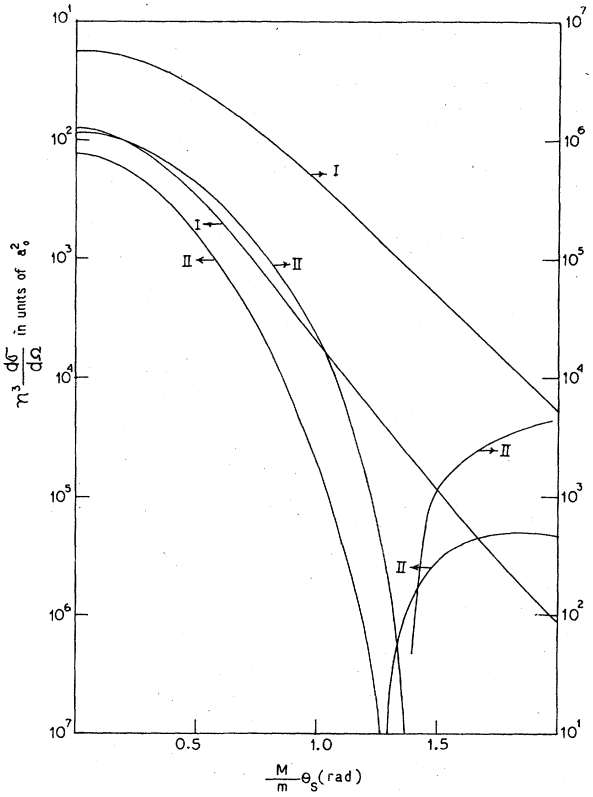

FIG. 5. n^3 differential cross section for $H^+ + H(ls) \rightarrow H(ns) + H^+$ when $n \rightarrow \infty$ for the small scattering angles at $E = 100$ keV and 5 MeV. Identification of curves are similar to Fig. 2.

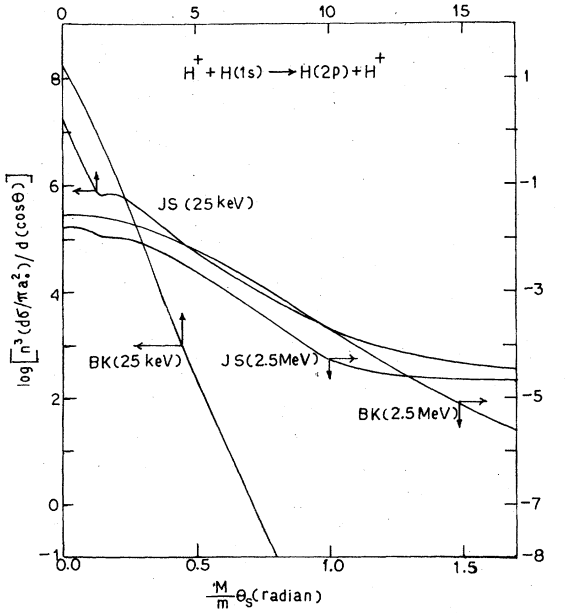

FIG. 6. JS and BK differential cross section $n^3\, d\sigma_{np}^{H}/d(\cos\theta_s)$ in units of πa_0^2 for the electron capture by protons from atomic hydrogen into the $2p$ state for projectile energies 25 keV and 2.5 MeV.

asymptotic differential cross sections for both the JS and BK have been shown for the incident energies 100 keV and 5 MeV. But Omidvar[7] in his asymptotic calculation has obtained the reverse feature, i.e., the zero of the differential curve is shifting away from the origin with the increase of the energy. In the high-energy limit the present result for the part of the asymptotic ($n \rightarrow \infty$) JS amplitude containing the internuclear distance is larger by a factor of 2 than the corresponding result of Omidvar as given in Eq. (28) of Ref. 7; the BK amplitude, however, is the same in both the calculations. Moreover, the approach to the high-energy limit is very slow and the contribution to the scattering amplitude of terms of order higher than $(1/v)^6$ is found to be quite significant in the energy range considered. Detailed investigation of this aspect of the asymptotic cross section will form the subject matter of a subsequent publication.

2. *s-p transition*

In Figs. 6 and 7 we display the present values of the differential cross section for $n = 2$ and $n = 5$, respectively, and that for the asymptotic case when $n \rightarrow \infty$ in Fig. 8, for incident energies 25 keV and 2.5 MeV. Unlike the case for $1s \rightarrow ns$ transition where a zero in the differential cross section is obtained at an intermediate scattering angle, the differential cross section for np capture does not exhibit any zero. Experimental measurements of the differential electron-capture cross section are extremely difficult owing largely to the highly forward-peaked character of the angular distribution. Only recently Cocke *et al.*[16] have measured the

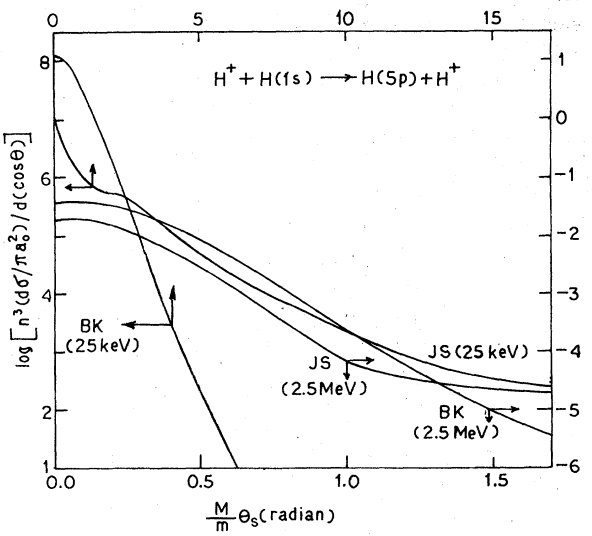

FIG. 7. Same as in Fig. 6, but for the electron capture into the $5p$ state.

TABLE I. Total n^3 cross sections (in πa_0^2) for the electron capture into ns ($n = 2$–$4, 6, 8, 10, 12, 14, 16, 18$) states of atomic hydrogen. The last column represents the asymptotic ($n \to \infty$) capture cross-section values.

E (keV)	n	2	3	4	6	8	10	12	14	16	18	∞
50	BK	4.487	4.657	4.710	4.745	4.757	4.762	4.765	4.767	4.768	4.769	4.772
	JS	0.6308	0.6568	0.6659	0.6724	0.6747	0.6757	0.6763	0.6766	0.6769	0.6770	0.6776
100	BK	0.5707	0.6090	0.6229	0.6330	0.6365	0.6382	0.6391	0.6396	0.6399	0.6402	0.6411
	JS	0.0933	0.0979	0.0996	0.1008	0.1012	0.1014	0.1016	0.1016	0.1017	0.1017	0.1018
200	BK [a]	3.522	3.723	3.796	3.850	3.869	3.877	3.882	3.885	3.887	3.888	3.893
	JS [a]	0.7396	0.7707	0.7820	0.7902	0.7930	3.7944	0.7951	0.7956	0.7959	0.7961	0.7968
400	BK [b]	1.239	1.285	1.301	1.313	1.317	1.319	1.320	1.321	1.321	1.322	1.323
	JS [b]	0.3376	0.3473	0.3507	0.3532	0.3541	0.3545	0.3548	0.3549	0.3550	0.3550	0.3553
600	BK [c]	1.459	1.498	1.512	1.522	1.526	1.528	1.529	1.529	1.529	1.530	1.531
	JS [c]	0.4563	0.4660	0.4695	0.4720	0.4729	0.4733	0.4735	0.4736	0.4737	0.4738	0.4740
1000	BK [d]	0.8693	0.8844	0.8898	0.8936	0.8950	0.8956	0.8960	0.8952	0.8963	0.8964	0.8967
	JS [d]	0.3161	0.3205	0.3221	0.3233	0.3237	0.3238	0.3239	0.3240	0.3240	0.3241	0.3242
2000	BK [e]	1.642	1.657	1.662	1.666	1.667	1.668	1.668	1.668	1.669	1.669	1.669
	JS [e]	0.7028	0.7082	0.7101	0.7115	0.7120	0.7122	0.7123	0.7124	0.7124	0.7124	0.7125
5000	BK [f]	0.7556	0.7584	0.7594	0.7601	0.7604	0.7605	0.7606	0.7606	0.7606	0.7606	0.7607
	JS [f]	0.3775	0.3787	0.3791	0.3794	0.3795	0.3796	0.3796	0.3796	0.3796	0.3796	0.3797

[a] All cross-section values are multiplied with 10^2.
[b] All cross-section values are multiplied with 10^3.
[c] All cross-section values are multiplied with 10^4.
[d] All cross-section values are multiplied with 10^5.
[e] All cross-section values are multiplied with 10^7.
[f] All cross-section values are multiplied with 10^9.

differential cross section for electron capture from argon by 6-MeV protons. They have not observed any zeros or minima in the differential cross section.

C. Integrated cross sections

1. s-s transition

Our computed results for the n^3 total capture cross sections into highly excited states ($n = 2$–$6, 8, 10, 12, 14, 16, 18$, and ∞) for the energy range 50 keV to 5 MeV have been tabulated in Table I. For all the discrete states from $n = 2$ to 18 the cross-section values are obtained with help of Eq. (5) along with Eqs. (27) and (32), whereas for the asymptotic cross section ($n \to \infty$) the limiting expressions as given by Eqs. (42) and (43) have been employed. It is of interest to note that at each incident energy the n^3-times cross section in a regular manner tends to a constant depending only on the energy with the increase of the value of n. From the table it is apparent that the values of n^3 cross sections for $n = 18$ are quite close to the corresponding asymptotic cross-section values at all energies. The n^{-3} law is thus satisfied throughout the energy range considered.

In order to test the postulated equality of the cross-section ratio introduced by Bates and Dalgarno[3]

$$\frac{\sigma_{\mathrm{JS}}^{\mathrm{H}}(1s \to ns)}{\sigma_{\mathrm{JS}}^{\mathrm{H}}(1s \to 1s)} = \frac{\sigma_{\mathrm{BK}}^{\mathrm{H}}(1s \to ns)}{\sigma_{\mathrm{BK}}^{\mathrm{H}}(1s \to 1s)},$$

we have tabulated our n^3 cross-section ratios for $n \to \infty$ in Table II. We have taken the ground-state capture-cross-section values of Chaudhuri *et al.*[5] to calculate the above ratios. For the high energy $E = 2000$ keV the two ratios R_1 and R_2 for BK and JS cross sections, respectively, agree rather well, the agreement becomes closer with the increase of the energy. The same scaleability of BK and JS in the limit of high energy thus seems to be reasonable.

TABLE II. Cross-section ratios $R_1 = n^3\sigma_{\mathrm{BK}}^{\mathrm{H}}(1s \to ns)/\sigma_{\mathrm{BK}}^{\mathrm{H}}(1s \to 1s)$[a] and $R_2 = n^3\sigma_{\mathrm{JS}}^{\mathrm{H}}(1s \to ns)/\sigma_{\mathrm{JS}}^{\mathrm{H}}(1s \to 1s)$[a] for $n \to \infty$.

E (keV)	50	100	200	400	1000	2000
R_1	1.4173	1.6068	1.4802	1.2970	1.1308	1.0699
R_2	1.3260	1.3888	1.3324	1.2210	1.1065	1.0573

[a] Calculated results of Chaudhuri *et al.* (Ref. 5) have been taken.

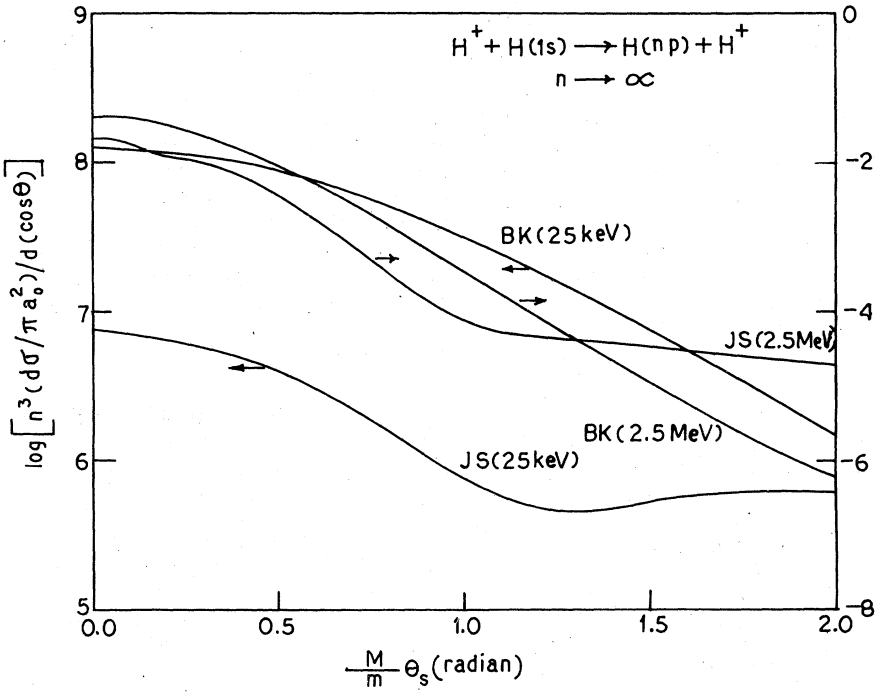

FIG. 8. Same as in Fig. 6, but for the electron capture into the *np* state, when $n \to \infty$.

In Table III we have also displayed the n^3 cross-section ratio values R_3 and R_5 defined as follows:

$$R_3 = \frac{n^3 \sigma^H_{BK}(1s \to ns)}{8\sigma^H_{BK}(1s \to 2s)} \quad \text{and} \quad R_4 = \frac{n^3 \sigma^H_{JS}(1s \to ns)}{8\sigma^H_{JS}(1s \to 2s)} .$$

From Table III it is evident that R_3 is very nearly equal to R_4 at high energies and for all energies considered the difference between R_3 and R_4 is much smaller than that between R_1 and R_2 of Table II. This behavior may be helpful for an estimate of the asymptotic JS cross section.

In Table IV we have tabulated the present cross-section ratios

$$R_5 = \sigma^H_{JS}(ns)/\sigma^H_{BK}(ns)$$

for various n values at several incident energies.

For comparison the available numerical values of the corresponding ratio due to Mapleton[14] for $2 \leq n \leq 5$ have also been included. Our present values are seen to be in excellent agreement with the available values of Mapleton.[17] For the high energy $E = 5$ MeV we obtain, when $n \to \infty$, the cross-section ratio value $R_5 \simeq 0.499$. The ratios R_5 for $n = 2$ and $n \to \infty$ at 5 MeV, the highest energy considered in Table IV, are very close to each other. We would like to point out that Omidvar[7] from his asymptotic calculations has obtained this ratio $R_5 \simeq 0.811$ for $n \to \infty$ and $E \to \infty$. From this table it is evident that present cross-section ratios for high incident energies are in close agreement with the corresponding values obtained by using the following relation of Jackson and Schiff[4] for capture into the ground state:

$$\frac{\sigma^H_{JS}(1s \to 1s)}{\sigma^H_{BK}(1s \to 1s)} = \frac{1}{192}\left[\left(27 + \frac{14}{E} + \frac{2}{E^2}\right) - 2A\left(83 + \frac{15}{E} + \frac{2}{E^2}\right) + 2A^2\left(31 + \frac{8}{E} + \frac{1}{E^2}\right)\right] ,$$

TABLE III. Cross-section ratios $R_3 = n^3\sigma^H_{BK}(1s \to ns)/8\sigma^H_{BK}(1s \to 2s)$ and $R_4 = n^3\sigma^H_{JS}(1s \to ns)/8\sigma^H_{JS}(1s \to 2s)$ for $n \to \infty$.

E (keV)	50	100	200	400	600	1000	2000	5000
R_3	1.0635	1.1236	1.1053	1.0678	1.0493	1.0315	1.0164	1.0067
R_4	1.0742	1.0915	1.0773	1.0524	1.0388	1.0256	1.0139	1.0058

TABLE IV. Ratio $\sigma_{JS}^{H}/\sigma_{BK}^{H}$ for $H^+ + H(1s) \rightarrow H(ns) + H^+$.

	E (keV)									
nl	50	100	200		400	600	1000	2000		5000
1s[a]	0.1544	0.1837	0.2278	0.228[b]	0.2323	0.3221	0.3697	0.4315	0.431[b]	0.4903
2s	0.1406	0.1634	0.2100	0.210[b]	0.2725	0.3127	0.3636	0.4280	0.430[b]	0.4996
3s	0.1410	0.1607	0.2070	0.207[b]	0.2703	0.3111	0.3624	0.4274	0.427[b]	0.4993
4s	0.1414	0.1598	0.2060	0.207[b]	0.2696	0.3105	0.3620	0.4273	0.425[b]	0.4992
$n \rightarrow \infty$	0.1420	0.1588	0.2047	•••	0.2686	0.3096	0.3615	0.4270	•••	0.4991

[a] Calculated results of Mapleton (quoted from Ref. 14).
[b] Calculated using Eq. (17) of Ref. 4.

where $A = \arctan(E^{1/2})/E^{1/2}$. For sufficiently high energies it is thus possible to obtain the JS cross section analytically employing the above relation and knowing the corresponding BK only.

2. *s-p transition*

In Table V we display our computed results for n^3 times the total capture cross sections $n^3\sigma_{np}^{H}$, for $n = 2-5, 8, 10, 12, 16, 20$, and ∞ for several incident energies from 25 keV to 2.5 MeV. It is of interest to note here that Eq. (5), along with Eqs. (37) and (40), have been employed to calculate the cross section for all the discrete states while Eqs. (35) and (36) have been used for the asymptotic case when $n \rightarrow \infty$. We see from the table that the cross-section values for $n = 20$ and $n \rightarrow \infty$ agree within an accuracy of 0.5% at all the energies considered. The values for $n^3\sigma_{np}^{H}$ reach a constant value in a regular manner and obey asymptotically the n^{-3} law as $n \rightarrow \infty$.

TABLE V. Capture cross sections $n^3\sigma_{np}^{H}$ is units of πa_0^2.

E (keV)	2	3	4	5	8	10	12	16	20	
I[a]	30.70	29.58	28.88	28.51	28.08	27.98	27.92	27.87	27.84	27.79
25.00										
II[b]	3.553	3.288	3.174	3.118	3.056	3.042	3.034	3.026	3.022	3.015
I	2.754	3.244	3.411	3.488	3.570	3.589	3.600	3.610	3.614	3.623
63.24										
II	0.4018	0.4497	0.4649	0.4716	0.4787	0.4803	0.4812	0.4821	0.4824	0.4832
I	0.2612	0.3199	0.3413	0.3513	0.3623	0.3648	0.3662	0.3676	0.3682	0.3694
112.46										
II[c]	4.733	5.581	5.876	6.013	6.161	6.195	6.214	6.232	6.241	6.256
I[c]	1.437	1.767	1.888	1.946	2.008	2.023	2.031	2.039	2.042	2.049
200.00										
II[c]	0.3251	0.3904	0.4138	0.4247	0.4365	0.4393	0.4408	0.4423	0.4429	0.4442
I[d]	0.5242	0.6397	0.6817	0.7014	0.7229	0.7279	0.7306	0.7333	0.7346	0.7368
355.60										
II[d]	0.1459	0.1756	0.1862	0.1912	0.1966	0.1978	0.1985	0.1992	0.1995	0.2000
I[e]	1.441	1.742	1.850	1.901	1.956	1.968	1.975	1.982	1.985	1.991
632.40										
II[e]	0.4796	0.5754	0.6095	0.6253	0.6426	0.6466	0.6488	0.6509	0.6520	0.6537
I[f]	0.3314	0.3976	0.4211	0.4320	0.4440	0.4468	0.4483	0.4498	0.4505	0.4517
1124.60										
II[f]	0.1277	0.1526	0.1614	0.1655	0.1700	0.1710	0.1716	0.1721	0.1724	0.1729
I[g]	6.835	8.159	8.627	8.845	9.081	9.135	9.165	9.194	9.208	9.232
2000.00										
II[g]	2.960	3.526	3.726	3.818	3.919	3.942	3.955	3.967	3.973	3.983
I[g]	1.490	1.776	1.877	1.924	1.975	1.987	1.993	1.999	2.002	2.008
2500.00										
II[g]	0.6701	0.7976	0.8425	0.8633	0.8860	0.8911	0.8940	0.8968	0.8981	0.9004

[a] I stands for BK results throughout.
[b] II stands for JS results throughout.
[c] All cross-section values are multiplied by 10^2.
[d] All cross-section values are multiplied by 10^3.
[e] All cross-section values are multiplied by 10^5.
[f] All cross-section values are multiplied by 10^6.
[g] All cross-section values are multiplied by 10^9.

TABLE VI. Cross-section ratios $R_5=n^3\sigma^{H}_{BK}(1s\rightarrow np)/\sigma^{H}_{BK}(1s\rightarrow 1s)$[a] and $R_6=n^3\sigma^{H}_{JS}(1s\rightarrow np)/\sigma^{H}_{JS}(1s\rightarrow 1s)$.[a]

E (keV)	63.24	112.46	200.0	355.6	632.4	1124.6	2000.0
R_5	2.0702	1.4046	0.7761	0.4004	0.2070	0.1091	0.0588
R_6	1.7012	1.2512	0.7391	0.3968	0.2075	0.1094	0.0588

[a] Calculated results of Mapleton (Ref. 14).

Table VI shows the present cross-section ratio values

$$R_5=\frac{n^3\sigma^{H}_{BK}(1s\rightarrow np)}{\sigma^{H}_{BK}(1s\rightarrow 1s)} \quad \text{and} \quad R_6=\frac{n^3\sigma^{H}_{JS}(1s\rightarrow np)}{\sigma^{H}_{JS}(1s\rightarrow 1s)}$$

as $n\rightarrow\infty$. From the table it is apparent that at $E=2$ MeV, the highest energy shown, the ratios R_5 and R_6 are identical in conformity with the postulate of Bates and Dalgarno.[3] Thus the same scaleability of the BK and JS cross sections in the high-energy limit for electron capture into np states holds good.

In Table VII we have also tabulated the n^3 times the asymptotic capture-cross-section ratios

$$R_7=\frac{n^3\sigma^{H}_{BK}(1s\rightarrow np)}{8\sigma^{H}_{BK}(1s\rightarrow 2p)} \quad \text{and} \quad R_8=\frac{n^3\sigma^{H}_{JS}(1s\rightarrow np)}{8\sigma^{H}_{JS}(1s\rightarrow 2p)}$$

as $n\rightarrow\infty$. A comparison of Tables VI and VII shows that, for $E=200$ keV, the relative difference between R_7 and R_8 is smaller than that between R_5 and R_6; while for 355 keV $<E\leq 2.5$ MeV the relative agreement between the latter ratios is better. Thus it seems that the Bates-Dalgarno equalities R_5 and R_6 may be more helpful for ascertaining the nature of the JS cross section in the limit of high energies. For $1s\rightarrow ns$ transition however it was noted that an estimate of the JS capture cross section could be made more conveniently with the help of

$$\frac{n^3\sigma^{H}_{BK}(1s\rightarrow ns)}{8\sigma^{H}_{BK}(1s\rightarrow 2s)}=\frac{n^3\sigma^{H}_{JS}(1s\rightarrow ns)}{8\sigma^{H}_{JS}(1s\rightarrow 2s)}$$

than by the Bates-Dalgarno equality.[3]

We give in Table VIII our cross-section ratios

$$R_9=\sigma^{H}_{JS}(np)/\sigma^{H}_{BK}(np)$$

for various n values at several incident energies. For $2p$ and $3p$ states, the ratios R_9 as computed by us are in excellent agreement with the corresponding ratios of Mapleton (not shown in the table) as quoted by McDowell and Coleman.[17] As evident from the table, at $E=2.5$ MeV the ratio R_9 for $n=2p$ is within an accuracy of 0.5% with that for the asymptotic case when $n\rightarrow\infty$. At this energy, our value for R_9 when $n\rightarrow\infty$ is 0.4484. Omidvar,[7] on the other hand, from his asymptotic calculation has obtained a value of this ratio $R_9\simeq 0.684$, for $n\rightarrow\infty$ in the limit of high energies.

D. Differential cross section

1. s-s transition

Figure 9 displays our results for the FBA differential cross section $d\sigma^{Ps}_{ns}/d\Omega$ for the Ps formation in excited $2s$ and $6s$ states at positron energies 50 and 100 eV. All the cross-section curves fall very sharply from a forward peak, become zero at an angle depending on the incident energy, and then rise again to a maximum to fall monotonically afterwards with the increase of the scattering angle. The zero in the differential cross section at an angle may be explained by the fact that the FBA scattering amplitudes for the attractive $1/r_1$ and the repulsive $1/r_2$ parts of the interaction potential cancel each other, being equal in magnitude but opposite in sign at this particular angle. For an idea of the relative orders of magnitude of attractive and repulsive interactions, we show in Table IX the contributions of each part of the scattering amplitude separately along with the differential cross sections at 200 eV for Ps formation in the $2s$, $8s$, and $12s$ states. The corresponding

TABLE VII. Cross-section ratios $R_7=n^3\sigma^{H}_{BK}(1s\rightarrow np)/8\sigma^{H}_{BK}(1s\rightarrow 2p)$ and $R_8=n^3\sigma^{H}_{JS}(1s\rightarrow np)/8\sigma^{H}_{JS}(1s\rightarrow 2s)$.

E (keV)	25.0	63.24	112.46	200.0	355.6	632.4	1124.6	2000.0	2500.0
R_7	0.9052	1.3156	1.4138	1.4262	1.4056	1.3814	1.3630	1.3507	1.3477
R_8	0.8486	1.2025	1.3217	1.3664	1.3714	1.3631	1.3540	1.3456	1.3437

TABLE VIII. Ratio $R_9 = \sigma_{TS}^{H}(np)/\sigma_{BK}^{H}(np)$ for $H^* + H(1s) \rightarrow H(np) + H^+$.

nl \ E (KeV)	25	63.24	112.5	200.0	355.6	632.4	1125	2000.0	2500.0
$2p$	0.1157	0.1459	0.1812	0.2230	0.2783	0.3328	0.3853	0.4331	0.4497
$3p$	0.1112	0.1386	0.1745	0.2209	0.2745	0.3303	0.3838	0.4321	0.4491
$4p$	0.1099	0.1363	0.1722	0.2192	0.2731	0.3295	0.3833	0.4319	0.4488
$5p$	0.1094	0.1352	0.1712	0.2182	0.2726	0.3289	0.3831	0.4317	0.4487
$16p$	0.1086	0.1335	0.1695	0.2169	0.2716	0.3284	0.3826	0.4315	0.4485
$n \rightarrow \infty$	0.1085	0.1334	0.1694	0.2168	0.2715	0.3283	0.3825	0.4313	0.4484

values of the asymptotic case are included in Table X for positron energies 50, 100, and 200 eV. It is evident from Table X that for all the n values considered, the two parts of the amplitude denoted by I_{n00} and J_{n00} become equal in magnitude at an angle around 24° and cancel each other. In the FBA, the same type of total cancellation of the attractive and repulsive parts of the amplitude also happens when Ps is assumed to be formed in the ground state. From Fig. 9 also it is apparent that the zero of the differential cross section for any particular incident energy occurs at almost the same angle for different s states. This angle is shifted from a higher value towards zero angle when we go on increasing the energy, and at higher energies the differential cross section peaks more sharply in the forward direction. We find from Table X that at 200 eV, about 90% of the total formation cross section in the $12s$ state comes from angles smaller than the angle at which the amplitude is exactly zero. The same is true for other s states also.

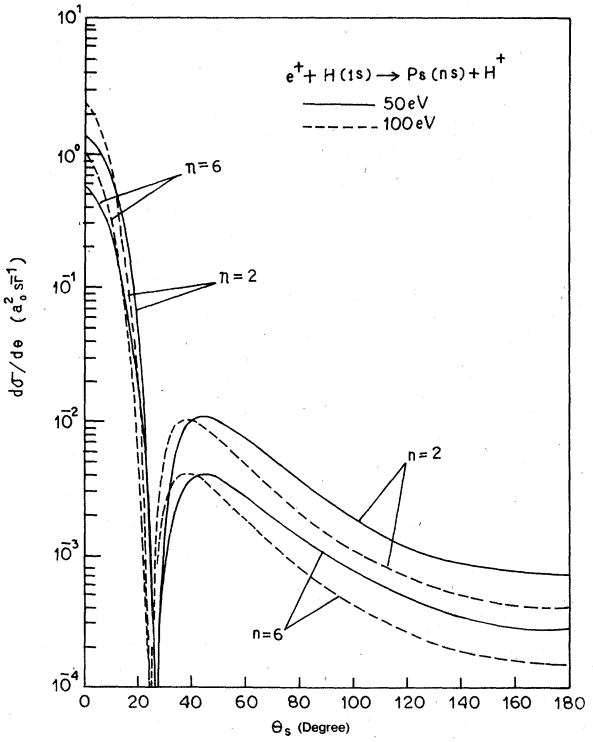

FIG. 9. Differential cross section $n^3 d\sigma_{n0}^{Ps}/d\Omega$ for positronium formation in the $2s$ and $6s$ excited states in positron–hydrogen-atom collisions for incident energies 50 and 100 eV.

In Fig. 10 we have plotted $n^3 d\sigma_{n\rightarrow\infty}^{Ps}/d\Omega$ for the asymptotic region when $n \rightarrow \infty$, at incident energies 20, 50, 100, and 500 eV. The zero in the differential cross section for the maximum energy 500 eV that we have considered, occurs at around 22°. This is not in agreement with the findings of Omidvar.[7] He has obtained by his asymptotic form of the scattering amplitude that $n^3 d\sigma_{n\rightarrow\infty}^{Ps}/d\Omega$ for $\theta_s \simeq 29°$ when the positron energy $k_i \gg 1$. We find for the asymptotic case, in conformity with our earlier observations for the s states, that the angle at which the differential cross section becomes zero moves with the impact energy. From a comparative study of the values of the attractive and the repulsive parts of the scattering amplitude from Table X, we observe that the asymptotic differential cross section becomes zero at around 42° for an incident positron energy 20 eV, while at 50 eV, this angle is shifted towards a smaller value around 27°. At an energy of 200 eV, the value of the angle is still smaller and is around 24°. We have given here only the rough estimates of these angles. The exact values may be calculated from the tabular points.

2. *s-p transition*

In Fig. 11, we display our values of the differential cross section $n^3 d\sigma_{np}^{Ps}/d\Omega$ for the states of $2p$ and $10p$ at the positron energy 100 eV only. The values for $n^3 d\sigma_{np}^{Ps}/d\Omega$ are found to fall monotonically with the increase of the scattering angle. They do not show any zero. This is due to the fact that the scattering amplitudes for the m-degenerate states attain zero values at different scattering angles and as a result, the total differential cross section neither becomes zero nor minimum at any stage.

TABLE IX. Differential cross sections $d\sigma^{Ps}/d\Omega$ ($a_0^2\,sr^{-1}$) for positronium formation in ns states and the scattering amplitudes I and J for the attractive and the repulsive potentials $1/r_1$, and $1/r_2$, respectively, at 200 eV.

Angle[a] (degree)	n = 2 $I\times10^{+2}$	2 $J\times10^{+4}$	2 DCS[b] $\times10^{+5}$	8 $I\times10^{+3}$	8 $J\times10^{+5}$	8 DCS $\times10^{+7}$	12 $I\times10^{+4}$	12 $J\times10^{+6}$	12 DCS $\times10^{+8}$	Total $\sigma_{12s}\times10^{+6}(\pi a_0^2)$
0.0	−11.67	2634.	1487.	−15.25	3420.	24521.	−83.17	18641.	7279.	
4.517	−10.34	2346.	1108.	−14.03	3037.	18221.	−76.50	16552.	5410.	0.8622
10.369	− 7.806	1486.	332.8	−10.27	1918.	541.9	−56.00	10453.	1608.	1.456
16.256	− 5.164	756.6	39.56	− 6.687	972.6	63.07	−36.45	5299.	187.0	1.564
22.150	− 3.340	353.8	0.2717	− 4.307	453.3	0.3485	−23.47	2469.	1.024	1.564
28.047	− 2.245	165.2	2.406	− 2.887	211.1	4.106	−15.73	1150.	12.20	1.576
33.946	− 1.598	80.26	4.238	− 2.039	102.3	7.038	−11.11	557.5	20.90	1.600
39.845	− 1.139	44.14	4.043	− 1.511	52.39	6.651	− 8.231	285.4	19.74	1.626
45.745	− 0.9111	22.33	3.244	− 1.166	28.40	5.312	− 6.353	154.7	15.76	1.650
51.645	− 0.7275	12.80	2.465	− 0.9302	16.27	4.023	− 5.068	88.60	11.94	1.669
57.546	− 0.5268	7.716	1.851	− 0.7626	9.801	3.016	− 4.154	53.38	8.949	1.684
63.447	− 0.5006	4.871	1.401	− 0.6394	6.184	2.278	− 3.483	33.68	6.760	1.607
69.347	− 0.4281	3.205	1.075	− 0.5465	4.068	1.747	− 2.977	22.16	5.184	1.707
75.250	− 0.3719	2.190	0.8405	− 0.4748	2.779	1.364	− 2.586	15.13	4.048	1.715
81.149	− 0.3279	1.548	0.6692	− 0.4184	1.964	1.086	− 2.279	10.70	3.221	1.721
87.050	− 0.2926	1.129	0.5427	− 0.3733	1.432	0.8799	− 2.033	7.801	2.611	1.727
92.950	− 0.2641	0.8477	0.4480	− 0.3368	1.075	0.7261	− 1.835	5.855	2.158	1.731
98.851	− 0.2407	0.6533	0.3761	− 0.3070	0.8283	0.6093	− 1.672	4.511	1.808	1.735
104.752	− 0.2214	0.5160	0.3208	− 0.2824	0.6541	0.5196	− 1.538	3.562	1.542	1.738
110.653	− 0.2054	0.4169	0.2778	− 0.2619	0.5285	0.4497	− 1.427	2.878	1.335	1.741
116.554	− 0.1921	0.3442	0.2440	− 0.2449	0.4363	0.3951	− 1.334	2.376	1.172	1.743
122.454	− 0.1809	0.2899	0.2173	− 0.2306	0.3675	0.3518	− 1.256	2.002	1.044	1.745
128.355	− 0.1716	0.2491	0.1960	− 0.2187	0.3157	0.3173	− 1.191	1.719	0.9415	1.746
134.255	− 0.1638	0.2179	0.1791	− 0.2088	0.2762	0.2898	− 1.137	1.504	0.8599	1.747
140.155	− 0.1678	0.1941	0.1656	− 0.2005	0.2459	0.2679	− 1.092	1.339	0.7949	1.748
146.054	− 0.1520	0.1758	0.1548	− 0.1938	0.2229	0.2505	− 1.055	1.213	0.7434	1.749
151.953	− 0.1477	0.1619	0.1464	− 0.1883	0.2052	0.2369	− 1.026	1.118	0.7030	1.750
157.850	− 0.1444	0.1516	0.1400	− 0.1841	0.1920	0.2266	− 1.003	1.046	0.6722	1.750
163.744	− 0.1419	0.1442	0.1353	− 0.1809	0.1827	0.2190	− 0.9855	0.9948	0.6497	1.751
169.631	− 0.1402	0.1392	0.1322	− 0.1787	0.1764	0.2139	− 0.9737	0.9610	0.6346	1.751
175.483	− 0.1393	0.1366	0.1305	− 0.1776	0.1731	0.2111	− 0.9673	0.9427	0.6264	1.751

[a] The angles correspond to 30 Gauss-Legendre quadrature points. The zero degree however does not belong to this family of quadrature points.
[b] Differential cross section.

TABLE X. Differential cross sections $n^3 d\sigma^{Ps}/d\Omega_{n\to\infty}(a_0^2\,\mathrm{sr}^{-1})$ for positronium formation in positron-hydrogen collisions for the asymptotic case when $n\to\infty$ and the scattering amplitudes $n^{3/2}I$ and $n^{3/2}J$ for the attractive and the repulsive potentials $1/r_1$ and $1/r_2$, respectively, at 50, 100, and 200 eV.

Angle[a] (degree)	E (eV) $n^{3/2}I$	50 $n^{3/2}J\times10^{+2}$	DCS[b] $\times10^{+2}$	$n^{3/2}I\times10^{+1}$	100 $n^{3/2}J\times10^{+3}$	DCS $\times10^{+3}$	$n^{3/2}I\times10^{+2}$	200 $n^{3/2}J\times10^{+4}$	DCS $\times10^{+4}$
0.0	−6.332	1075.	1177.	−18.68	3590.	1949.	−34.62	7758	1260
4.517	−6.034	1009.	994.2	−17.41	3263.	1524.	−31.84	6888	936.3
10.370	−4.981	782.3	487.4	−13.28	2241.	547.4	−23.31	4349	278.2
16.256	−3.704	519.8	134.8	− 8.920	1262.	86.74	−15.17	2205	32.33
22.150	−2.621	314.2	16.40	− 5.905	647.3	2.123	− 9.765	1027	0.1759
28.047	−1.844	182.0	0.0349	− 3.970	325.4	3.370	− 6.545	478.5	2.114
33.946	−1.323	104.7	4.596	− 2.787	167.0	8.200	− 4.621	231.9	3.618
39.456	−0.9783	61.12	8.132	− 2.048	89.21	8.775	− 3.424	118.7	3.417
45.745	−0.7476	36.64	8.765	− 1.566	49.92	7.488	− 2.642	64.34	2.728
51.645	−0.5892	22.68	7.922	− 1.240	29.29	5.901	− 2.108	36.85	2.066
57.456	−0.4772	14.51	6.652	− 1.010	17.97	4.537	− 1.728	22.20	1.548
63.447	−0.3958	9.603	5.422	− 0.8431	11.50	3.484	− 1.449	14.01	1.169
69.347	−0.3351	6.560	4.383	− 0.7176	7.653	2.701	− 1.238	9.214	0.8969
75.248	−0.2888	4.619	3.552	− 0.6214	5.275	2.125	− 1.076	6.294	0.7003
81.149	−0.2528	3.347	2.903	− 0.5461	3.756	1.700	− 0.9480	4.449	0.5572
87.050	−0.2243	2.409	2.399	− 0.4862	2.755	1.382	− 0.8458	3.244	0.4516
92.950	−0.2015	1.901	2.008	− 0.4379	2.078	1.144	− 0.7632	2.435	0.3726
98.851	−0.1829	1.485	1.704	− 0.3985	1.607	0.9614	− 0.6956	1.876	0.3127
104.752	−0.1677	1.186	1.465	− 0.3661	1.274	0.8208	− 0.6398	1.481	0.2667
110.653	−0.1551	0.9681	1.267	− 0.3393	1.032	0.7113	− 0.5935	1.197	0.2309
116.554	−0.1447	0.8059	1.126	− 0.3169	0.8540	0.6251	− 0.5549	0.9881	0.2028
122.454	−0.1360	0.6837	1.006	− 0.2983	0.7209	0.5568	− 0.5226	0.8325	0.1805
128.345	−0.1287	0.5907	0.9105	− 0.2827	0.6202	0.5025	− 0.4956	0.7150	0.1629
134.255	−0.1227	0.5193	0.8334	− 0.2697	0.4534	0.4590	− 0.4731	0.6255	0.1488
140.155	−0.1170	0.4644	0.7717	− 0.2589	0.4845	0.4244	− 0.4544	0.5570	0.1376
146.054	−0.1137	0.4221	0.7227	− 0.2501	0.4393	0.3969	− 0.4391	0.5046	0.1286
151.953	−0.1104	0.3898	0.6841	− 0.2431	0.4049	0.3754	− 0.4267	0.4648	0.1216
157.850	−0.1078	0.3657	0.6546	− 0.2375	0.3793	0.3589	− 0.4171	0.4350	0.1163
163.744	−0.1059	0.3483	0.6331	− 0.2334	0.3608	0.3469	− 0.4099	0.4137	0.1124
169.631	−0.1046	0.3368	0.6186	− 0.2305	0.3487	0.3389	− 0.4050	0.3996	0.1098
175.483	−0.1039	0.3306	0.6107	− 0.2290	0.3421	0.3345	− 0.4023	0.3920	0.1083

[a] The same as in Table IX.

[b] Differential cross section.

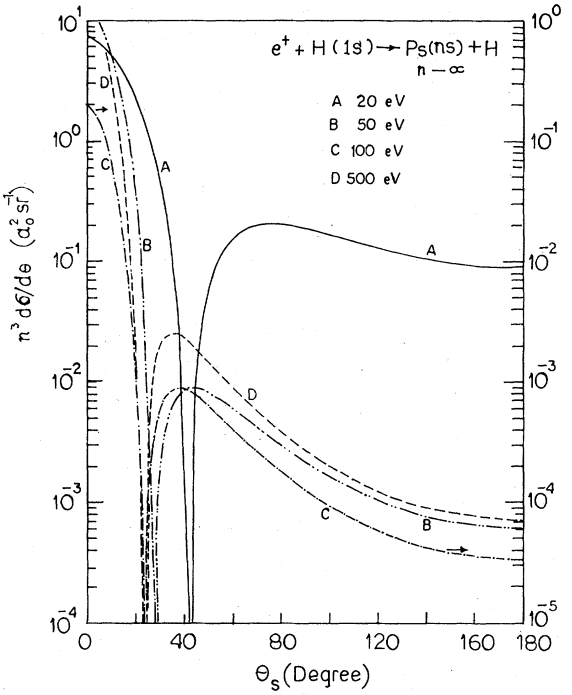

FIG. 10. Asymptotic differential cross section $n^3\, d\sigma/d\Omega$ as $n \rightarrow \infty$ for positronium formation in positron–hydrogen-atom collisions for energies 20, 50, 100, and 500 eV.

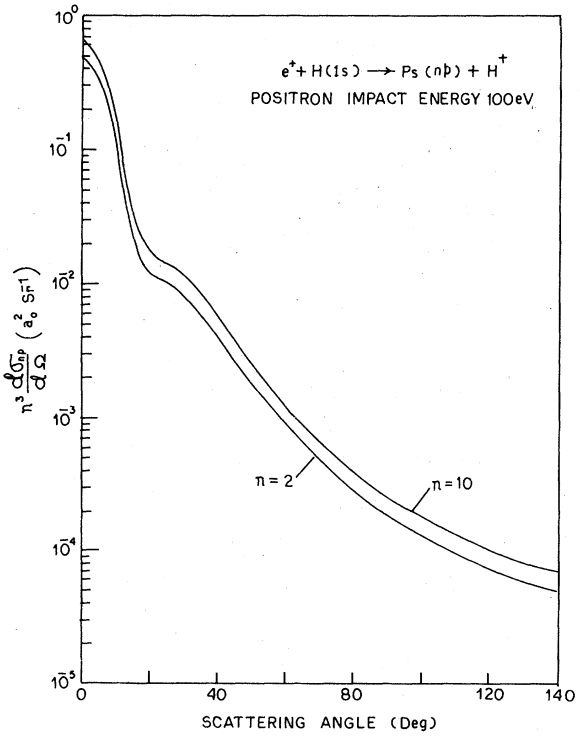

FIG. 11. Differential cross section $n^3\, d\sigma/d\Omega$ in units of πa_0^2 for the positronium formation into the $2p$ and $10p$ states in positron–hydrogen-atom collisions for the positron energy 100 eV.

TABLE XI. Total cross section in units of πa_0^2 for the positronium formation in ns excited states in positron-hydrogen collisions using the first Born approximation. The numbers give the n^3-times cross-section values.

E (eV) \ n	2	3	4	5	6	7	8	9	10	11	12	13	14	15	16	17	18
20	1.8218	1.4831	1.3659	1.3123	1.2833	1.2659	1.2547	1.2470	1.2415	1.2374	1.2343	1.2319	1.2300	1.2285	1.2272	1.2262	1.2253
50	0.5152	0.5347	0.5379	0.5393	0.5400	0.5405	0.5407	0.5409	0.5411	0.5412	0.5413	0.5414	0.5414	0.5414	0.5415	0.5415	0.5415
100 [a]	0.5496	0.5687	0.5755	0.5787	0.5804	0.5815	0.5822	0.5826	0.5830	0.5832	0.5834	0.5836	0.5837	0.5838	0.5838	0.5839	0.5840
200 [a]	0.2887	0.2966	0.2994	0.3007	0.3014	0.3018	0.3021	0.3023	0.3024	0.3025	0.3026	0.3027	0.3027	0.3028	0.3028	0.3028	0.3028
500 [a]	0.2966	0.3008	0.3023	0.3030	0.3034	0.3036	0.3038	0.3039	0.3039	0.3040	0.3040	0.3041	0.3041	0.3041	0.3041	0.3041	0.3041

[a] The values for 100, 200, and 500 eV should be multiplied by 10^{-1}, 10^{-2}, and 10^{-4}, respectively.

E. Total cross section

1. s-s transition

In Table XI we show our results for n^3 times the total integrated cross section $n^3\sigma_{ns}^{Ps}$ for Ps formation in ns states, n ranging from 2 to 18, at several incident positron energies from 20 to 500 eV. Our cross-section value for the Ps formation in the 2s excited state at 20 eV is the same as that predicted by Massey and Mohr[11] previously. The values of $n^3\sigma_{ns}^{Ps}$ are found to be close to one another for $n \geq 8$ at all energies considered. As the value of the principal quantum number n is increased, $n^3\sigma_{ns}^{Ps}$ tend to become a constant depending on the energy alone. In other words, it can be concluded that the total Ps-formation cross section satisfies the n^{-3} law irrespective of the positron impact energy.

The values of $n^3\sigma_{n\to\infty}^{Ps}$ are shown in Table XII. Beyond 20 eV, the values fall at a faster rate. By comparison of these two sets of results it is seen that, at all energies considered, the asymptotic value for the cross section is reached within an accuracy of 1% when the excited state is an 18s state. Beyond this state, therefore, $n^3\sigma_{ns}^{Ps}$ gives almost its asymptotic value $n^3\sigma_{n\to\infty}^{Ps}$ at all energies above 20 eV.

2. s-p transition

Table XIII shows our results for n^3 times the total cross section $n^3\sigma_{np}^{Ps}$ for the Ps formation in the np states. There exists, to our knowledge, no other previous calculation for the Ps formation in np states. We have computed the cross section for the excited states $n=2$–6, 10, 16, and ∞ at incident energies 20, 50, 100, 200, and 500 eV. It is apparent from the table that $n^3\sigma_{np}^{Ps}$ tends to become a constant with the increase of n for all the positron energies considered. We also note that the values of $n^3\sigma_{np}^{Ps}$ for $n=16$ and $n\to\infty$ are within 0.5% at all energies. Thus the n^{-3} law for the cross section is seen to be satisfied here in the limit of large n irrespective of the projectile energy.

TABLE XII. Asymptotic positronium-formation cross section $n^3\sigma_{n\to\infty}^{Ps}$ in positron–hydrogen-atom scattering.

E (eV)	$n^3\sigma_{n\to\infty}(\pi a_0^2)\times 10^4$
20	12180.8
50	5416.9
100	584.41
200	30.303
500	0.30425

V. CONCLUSION

In this work, we have given a new technique to evaluate the FBA scattering amplitude for the general rearrangement collisions in which the final bound state may be formed in arbitrary excited ns and np states. We have applied this amplitude to compute differential and total cross sections for the electron capture by protons and positrons from atomic hydrogen in its normal state for various projectile energies. The asymptotic form of the scattering amplitude as $n\to\infty$ may be obtained by our method without encountering any further difficulties.

The evaluation of the scattering amplitude involves a contour integration for which we have taken a circular path. The radius of the circular contour has been chosen conveniently so that the numerical evaluation causes no problem at all and does not require much computer time. This approach will be helpful to ascertain the behavior of the cross section for electron capture into any excited states as well as for the asymptotic capture cross section as $n\to\infty$.

For capture into highly excited, the n^{-3} law for the FBA cross section is found to be satisfied irrespective of the kind of projectile and its incident energy. We also find that for the s-state capture, the zero of the FBA differential cross section occurs at an angle depending on the pro-

TABLE XIII. Total cross section $n^3\sigma_{np}^{Ps}$ in units of πa_0^2 for the positronium formation in np states in positron–hydrogen-atom collisions.

Energy (eV) \ n	2	3	4	5	6	10	16	∞
20	1.7802	1.7824	1.7656	1.7550	1.7485	1.7381	1.7344	1.7319
50	0.2340	0.2719	0.2846	0.2903	0.2935	0.2980	0.2995	0.3005
100[a]	1.484	1.787	1.895	1.945	1.973	2.013	2.027	2.035
200[b]	4.205	5.077	5.389	5.535	5.615	5.731	5.771	5.797
500[c]	1.760	2.108	2.232	2.290	2.322	2.367	2.383	2.393

[a]All cross-section values are multiplied by 10^{+2}.
[b]All cross-section values are multiplied by 10^{+4}.
[c]All cross-section values are multiplied by 10^{+6}.

jectile energy. The position of this angle is shifted towards the forward direction with the increase of the energy and the differential cross section peaks more sharply. This angle does not depend on the value of the principal quantum number n.

Our total cross-section values for the low-lying discrete states in proton–hydrogen-atom collisions show excellent agreement with the previous findings of Mapleton and of Band; and the cross-section ratios R_1 and R_2 favor the cross-section ratio equality of Bates and Dalgarno in conformity with the calculation of Mapleton. The smooth regular behavior of n^3 times the total cross section with increasing n and the closeness within 0.5% of the results for $n=20$ and $n\to\infty$ do certainly confirm the reliability and the suitability of the present method of calculation.

The reported results for the Ps formation in arbitrary excited ns and np states are quite new. And as there are no other theoretical as well as experimental findings for the process, any comparative study is not possible.

[1]J. R. Oppenheimer, Phys. Rev. 31, 349 (1928).
[2]H. C. Brinkman and H. A. Kramers, Proc. Acad. Sci. (Amst.) 33, 973 (1930).
[3]D. R. Bates and A. Dalgarno, Proc. Phys. Soc. A 66, 972 (1953).
[4]J. D. Jackson and H. Schiff, Phys. Rev. 89, 359 (1953).
[5]D. R. Bates, Proc. R. Soc. A 247, 294 (1958). R. S. Bassel and E. Gerjouy, Phys. Rev. 117, 749 (1960). M. R. C. McDowell, Proc. R. Soc. A 264, 277 (1961). I. M. Cheshire, Proc. Phys. Soc. Lond. 83, 227 (1964). R. McCarroll and A. Salin, Proc. R. Soc. A 300, 202 (1967). D. F. Gallaher and L. Wilets, Phys. Rev. 169, 139 (1968). J. C. Y. Chen and P. J. Kramer, Phys. Rev. A 5, 1207 (1972). J. Chaudhuri, A. S. Ghosh, and N. C. Sil, Phys. Rev. A 7, 1544 (1973).
[6]M. B. McElroy, Proc. R. Soc. A 272, 542 (1963). A. S. Ghosh, and N. C. Sil, J. Phys. B 4, 836 (1971). N. C. Sil, J. Chaudhuri, and A. S. Ghosh, Phys. Rev. A 12, 785 (1975). H. P. Saha, J. Chaudhuri, and N. C. Sil, Phys. Rev. A 14, 2373 (1976).
[7]K. Omidvar, Phys. Rev. A 12, 911 (1975).
[8]I. C. Pericval and D. Richards, in *Advances in Atomic and Molecular Physics*, edited by D. R. Bates and B. Bederson (Academic, New York, 1975), Vol. 11, p. 1.
[9]H. W. Kendal, Ph.D. thesis (MIT, 1954) (unpublished); E. R. Carlson, Bull. Am. Phys. Soc. 18, 1512 (1973); S. L. Verghese, E. S. Ensberg, V. M. Hughes, and I. Lindgren, Phys. Lett. A 49, 415 (1974); K. F. Canter, A. P. Mills, Jr., and S. Berko, Phys. Rev. Lett. 33, 7 (1974); 34, 177 (1975); and (erratum) 34, 848 (1975).
[10]A. P. Mills, S. Berko, and K. F. Canter, Phys. Rev. Lett. 34, 1541 (1975).
[11]H. S. W. Massey and C. B. O. Mohr, Proc. Phys. Soc. A 67, 695 (1954).
[12]R. Courant and D. Hilbert, *Methods of Mathematical Physics* (Interscience, New York, 1953), Vol. I, p. 509. There is however a difference of a factor $n!$ between our definition and that given by these authors. It arises from the choice of a different normalization constant for the wave function.
[13]R. R. Lewis, Jr., Phys. Rev. 102, 537 (1956), Eqs. (1)–(10) of Appendix I.
[14]R. A. Mapleton, Phys. Rev. 126, 1477 (1962).
[15]Y. B. Band, Phys. Rev. A 8, 2857 (1973); 8, 2866 (1973).
[16]C. L. Cocke, J. R. Macdonald, B. Curnutte, S. L. Varghese, and R. Randal, Phys. Rev. Lett., 36, 782 (1976).
[17]M. R. C. McDowell and J. P. Coleman, *Ion-Atom Collisions* (North-Holland, Amsterdam, 1970), p. 384.